Reconstructing surface wave profiles from forward scattered pulses

Sean P. Walstead and Grant B. Deane
Scripps Institute of Oceanography
Univ. of California, San Diego
La Jolla, CA. USA
Email: swalstead@ucsd.edu

Abstract— **Surface wave shape is determined by analyzing underwater reflected acoustic signals collected at multiple receivers in a wave tank. The acoustic signals are short 3-cycle pulses of nominal frequency 300 kHz. With the use of a forward scattering model based on the Kirchhoff approximation, an inverse processing algorithm determines surface wave shape by matching model and data acoustic waveforms. Reconstructed surfaces are accurate to a resolution of about a quarter-wavelength of the acoustic pulse only within Fresnel zones associated with each source and receiver pair. Within Fresnel zone regions, the acoustically derived surface is known with greater certainty than the surface profile as measured with a camera. Multiple receivers extend the region of surface reconstructed acoustically. The type of wave features to be investigated by this technique is scalable with acoustic transmission frequency. This versatility in implementation leads to the prospect of ocean application across a wide range of length scales.**

Keywords—remote sensing; rough interface scattering; inversion; underwater acoustics

I. INTRODUCTION

The problem of wave scattering from rough surfaces has received considerable attention in recent decades. The effect of surface roughness on electromagnetic wave scattering has application for example to land and sea radar design, and also is involved in astronomy and optics studies. More recently, the scattering of acoustic waves from rough surfaces has seen application in areas such as ultrasonic imaging and crack detection in structural engineering building design. In the ocean context, rough surface acoustic scattering is typically focused on bottom sediment scattering, object (e.g. fish) scattering, and air-sea interface scattering. The study presented in this paper is concerned with the later of those topics, namely underwater acoustic scattering from surface gravity waves.

Interest in acoustic wave scattering from the sea surface is motivated by recent studies that have shown during swell-dominated, low wind conditions, the sea surface acts like a lens, producing spatially and temporally highly focused regions of acoustic energy [1]. Fluctuations in surface reflected acoustic energy due to a non-stationary overhead wave field are not easily predicted and hence degrade the performance of underwater acoustic communication systems [2]. Focused acoustic signals from surface gravity waves are highly sensitive to details of the reflecting surface. This leads to the prospect of inversely solving for wave shape based on the form of forward scattered acoustic pulses.

Walstead and Deane [3] have already shown that surface wave shape can be determined by analyzing forward scattered acoustic pulses in a wave tank. In that study, two fundamental length scales intrinsic to the inversion process are confirmed. An outer length, on the order of a Fresnel zone surrounding a specular reflection point, is the only region of the surface that can be deduced acoustically to within a resolution set by the inner length of $\lambda_0/4$ where λ_0 is the dominant wavelength of the acoustic pulse. Those length scales provide a framework for the amount of information about a reflecting surface that can be extracted from a forward scattered pulse.

The inversion process developed in [3] and adapted in this study involves a cost function minimization which seeks to match model forward scattered acoustic pulses with those detected at a receiver. The forward scattering model, based on earlier work by Berry [4], is able to numerically simulate received acoustic waveforms for a specified reflecting surface $\eta(x)$ where x is the horizontal position between source and receiver. The fact that $\eta(x)$ only depends on one spatial dimension implies that uniformity has been assumed in the along-crest direction.

Numerical simulations of wave scattering from rough surfaces are either carried out exactly by solving an integral equation or approximately by making certain assumptions about the roughness of the surface. The two most common approximations in solving the rough surface scattering problem are the perturbation approximation and the Kirchhoff, or tangent plane approximation. See for instance Oglivy [5] for an extensive review of those approximate techniques. The modeling work employed in the current study makes use of the Kirchhoff approximation as it is particularly amenable to high frequency wave scattering. Whereas the perturbation approach is valid when the root-mean-square (rms) surface height is small compared to the acoustic wavelength, the Kirchhoff approximation is valid when the radius of curvature

This work has been supported by the Office of Naval Research (Grant No. N00014-11-1-0158) and the National Science Foundation (Grant No. OCE-1061050).

978-0-933957-40-4

is large compared to an acoustic wavelength [6]. Use of the Kirchhoff approximation results in considerably faster computation time. Care must be taken however that certain wave scattering effects are not important such as multiple reflection within a wave crest or shadowing by highly sloped surfaces with regard to grazing angle as these effects are neglected when the Kirchhoff approximation is employed.

The wave shape inversion experiment outlined in this study and in [3] occurs in a wave tank that is scaled to model an open ocean scenario. The ultimate goal of this inversion work is to apply the process to an open ocean data set. The motivation for the current experiment is to improve the robustness of the inversion process to ready the procedure for ocean application. Several key changes have been made to the inverse processing approach presented in [3] and are discussed in Sec. III. In order to overcome the outer length scale on surface wave reconstruction, multiple (four) receiver hydrophones are used. Also a camera is used to verify the inversion results. Results and discussion of the current experiment are presented in Sec. IV. Lastly, remarks about the versatility and usefulness of this acoustic remote sensing technique are included in the conclusion Sec. V.

II. THE EXPERIMENT

The experiment took place in a 33-m long glass walled wave tank at the Hydraulics lab at Scripps Institute of Oceanography. The wave tank was 0.6 m wide and 0.59 m deep. A schematic of the experimental setup is shown below in Fig. 1. Non-periodic wave packets were generated by a hydraulically driven paddle upstream of the acoustic system. Five high frequency transducers (International Transducer Corp. ITC 1089Ds) with a bandwidth of 100-300 kHz were mounted in the tank. One transducer acted as the acoustic source, while the other four were used as receivers. The separation between source and receiver R0 is 1.2 m, while the separation between each of the receivers is about 0.3 m. The depth of all transducers is 0.355 m. Transducers were oriented 45^o with regard to the wave channel bottom and positioned along the center-line of the tank.

A high speed camera, the 1.3 megapixel MotionPro x3, was used to provide ground-truth measurements of the overhead surface wave field. Pulse transmission and data acquisition occurred at a sampling rate of 2 MS/s. Successive acoustic pulses were transmitted for a duration of about 1.5 sec at a rate of about 37 Hz. The transmit pulses were short 3-cycle water pressure pulses with a nominal frequency of about 300 kHz.

The inverse processing is very sensitive to small changes in source and receiver position. Thus, the source and receiver geometry is determined from a damped least-squares nonlinear optimization using direct and reference flat-surface reflected acoustic arrival times. The sound speed, as measured by a micro-CTD, was 1523.2 m/s.

III. INVERSION PROCEDURE

The inverse processing scheme used to determine surface wave shape is the same as in [3] with slight modifications. Although the processing scheme will be briefly overviewed here, interested readers should consult Appendix C. of [3] for a complete description of the inversion algorithm. Overall, the inverse algorithm seeks to find a surface wave profile that results in model scattered pulses that match the received data pulses. Goodness of match between model and data is described by a cost function based on the residuals between the two pulses. During each iteration of the inverse process, a candidate surface wave profile is adjusted slightly so that the model and data pulses are better matched, and the cost function value is reduced. The next iteration uses that modified candidate surface wave profile as a starting estimate and makes another new adjustment to the wave profile. Once the cost function has been minimized to a level set by the experimental noise, no further adjustments to the wave field are made and the surface displacement profile that remains is

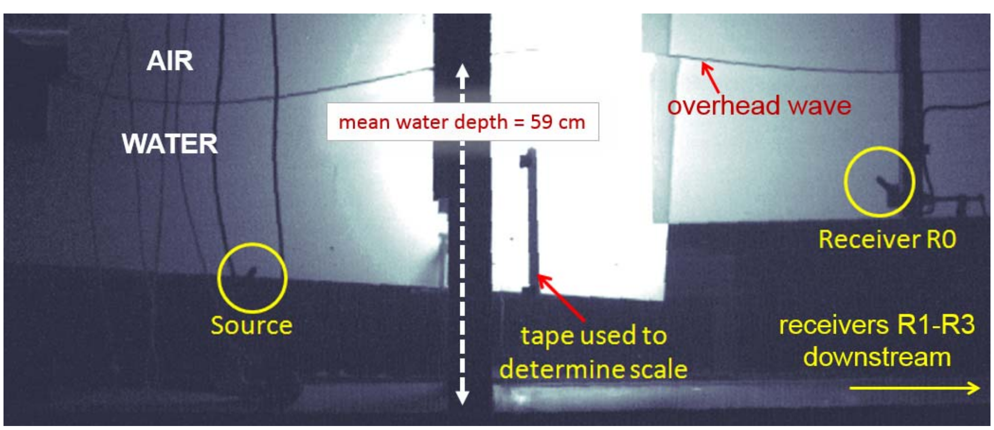

Fig. 1. Camera image of the experimental setup. Note that the transducer positions depicted in this image are slightly different than the transducer positions when data collection occurred. Although the field of view of the camera only captures the most upstream receiver R0, most specular reflection points lie between the source and receiver R0. The overhead wave propagates from left to right in the figure.

considered the reconstructed surface wave.

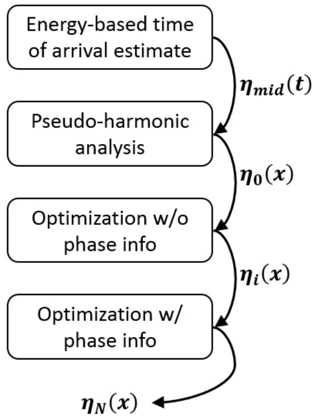

Fig. 2. Overview of the inversion procedure. $\eta_N(x)$ represents the reconstructed surface wave profile.

A schematic of the inversion algorithm is shown in Fig. 2. An initial starting wave profile is required for the iterative inverse processing. In order to generate that profile, first the surface elevation time series corresponding to midway between source and receiver $\eta_{mid}(t)$ is computed using time of arrival values of the surface reflected pulses. From that surface elevation time series, an initial spatial wave profile $\eta_0(x)$ is generated using pseudo-harmonic analysis. Pseudo-harmonic analysis (see Appendix B of [1]) assigns phase delays to each spectral component of the surface wave spectrum according to the linear dispersion relation allowing spatial surface elevation to be computed from a temporal record of surface elevation. Once the initial surface profile is specified, the inverse processing routine is first performed ignoring the phase information of the model and data pulses. This improves the robustness of the inversion algorithm to handle cases where the initial model waveform is more than one wavelength apart in delay time from the data waveform. If this step is ignored and phase information is initially considered, the inverse algorithm may converge on local solutions that represent model and data pulses that are an integer number of wavelengths apart in delay time. Once this first round of the inversion is complete, indicated by the cost function reaching its termination threshold, the inverse processing is repeated again but using the phase information of the waveforms. After the cost function is reduced this second time to its termination threshold, the iterative optimization terminates, no further adjustments are made to the surface displacement profile, and $\eta_N(x)$ is considered the reconstructed surface wave profile.

IV. RESULTS AND DISCUSSION

Reconstructed surface wave profiles are generated from surface reflected acoustic pulses for 50 consecutive instances. In 41 of the 50 pulses analyzed, the cost function was reduced below the noise threshold. The 9 cases in which cost function was not reduced below the noise threshold are attributed to data collection during especially noisy periods.

Acoustic data and forward model waveforms for pulse 17 are shown in Fig. 3. Only data from receiver R2 is shown as data from receivers R0, R1, and R3 are similar. The waveform generated from the initial surface wave profile has an arrival time that is about 4 µs greater than the arrival time of the data pulse. Assuming that each pulse originates from the same specular reflection point, the total path length between data pulse and initial model pulse is thus in error by about 6.1 cm. It is the job of the inversion algorithm to correct for this discrepancy and properly match the model pulse to data pulse with regard to both time of arrival and amplitude. The model waveform generated from the optimized profile shown in light red indeed correctly matches the data pulse in terms of both time of arrival and amplitude.

The reconstructed surface wave profile derived from acoustic pulse 17 is shown in Fig. 4. Also depicted is the initial surface profile and the camera data. Surrounding the optimized or reconstructed surface profile is a 1-σ confidence region which has been computed by a statistical analysis of the optimization parameters (see Appendix B of [3]). Fresnel zones denoted by the bars above and below the reconstructed

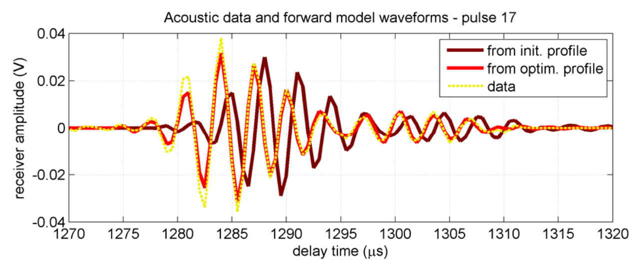

Fig. 3. Acoustic data and forward model waveforms for pulse 17. The dashed line represents the data collected at receiver R2. Similar waveforms are observed at receivers R0, R1, and R3. The model waveform generated from the initial surface profile (dark line) is about 1.3 wavelengths apart from the data pulse in delay time. The model waveform generated from the optimized profile (light line) is well matched with the data pulse in terms of arrival time and amplitude.

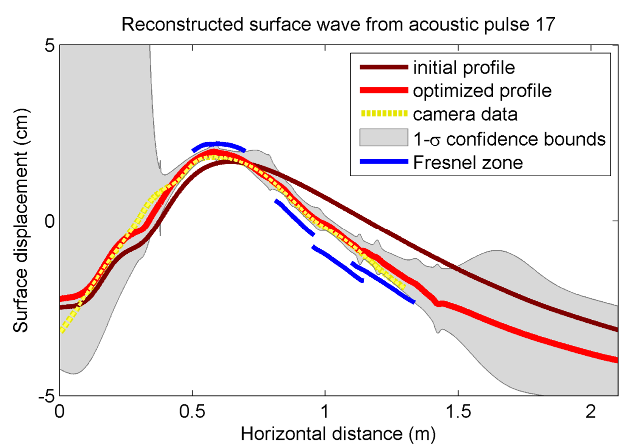

Fig. 4. Reconstructed surface wave from acoustic pulse 17. The blue bars above and below the surface wave profiles represent the Fresnel zones surrounding each specular reflection point associated with receiver R0-R3 from left to right. Camera data shown in the dashed line does not extend past 1.3 m in horizontal distance because of the limited field of view of the camera.

surface wave profile indicate the location of specular reflection points for each receiver. A Fresnel zone is defined as the extent of surface surrounding each specular reflection point where individual component reflected pulses have a phase difference of less than $\pi/2$ as compared to the specular reflection.

The statistical confidence in the surface profile is greatest within Fresnel zone regions. Each Fresnel zone is on the order of $50\lambda_0$. By using four receivers instead of one, the extent of surface reconstructed acoustically has increased by about a factor of four to $100\lambda_0$. Within Fresnel zone regions of the surface, the 1-σ confidence in the surface reconstruction approaches the inner length scale of $\lambda_0/4$. The camera data agrees very well with the optimized estimate of the surface wave profile. Because of parallax error and some ensemble averaging of camera images, the camera data has a 1-σ confidence of about 6 mm. Thus within Fresnel zone regions, the acoustically derived surface is more accurate than the profile as measured by the camera. This highlights the great sensitivity of amplitude and phase information of a surface scattered pulse to details of the overhead wave shape.

The initial surface profile is in greatest error (as compared to the camera data) around a horizontal distance of 1 m which is in the Fresnel zone region for receiver R2. Not only is the surface elevation too great at this position, but the local radius of curvature also appears to be in error. In fact, the optimized surface displacement profile adjusts the surface elevation of the initial profile within the Fresnel zone region of R2 by about 8.5 mm. This corresponds to exactly the 6.1 mm change in path length required to correct for the mismatched arrival time in the wave forms shown in Fig. 3. While surface elevation affects the time of arrival between model and data pulse, the local radius of curvature accounts for discrepancies in amplitude between model and data pulse.

V. CONCLUSION

Surface wave shapes have been computed from underwater forward scattered acoustic pulses. The use of multiple receivers effectively increases the extent of surface that can be reconstructed acoustically. Statistical confidence in the optimized profiles is greatest within Fresnel zone regions (of average length $50\lambda_0$) surrounding specular reflection points. Also within Fresnel zone regions, the statistical confidence of the optimized surface profile approaches the inner length scale limit of $\lambda_0/4 \approx 1.3$ mm and exceeds the resolution of the camera used to provide ground-truth measurements of the overhead wave field.

The inversion algorithm is robust in two ways. First, initial surface profiles are generated from the acoustics alone and does not require additional instrumentation such as wave gauges or upward looking SONARS. Second, the inversion algorithm is able to reconstruct wave shape even if the initial surface profile is in error by more than an acoustic wavelength. Success in determining wave shape along with

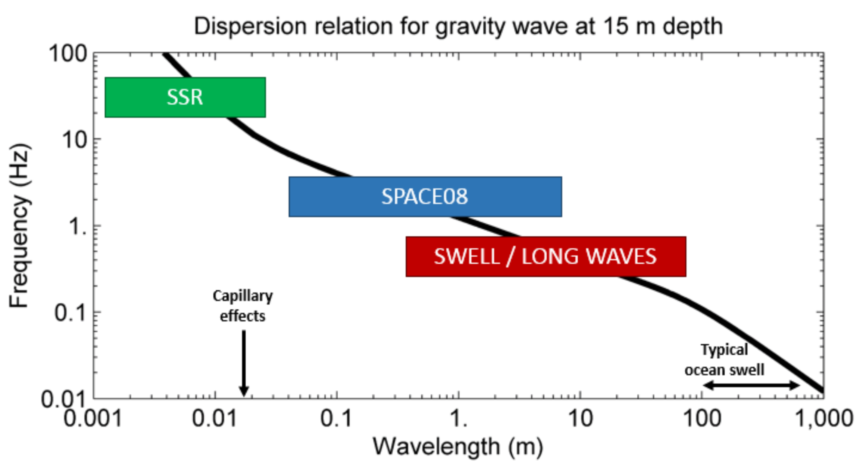

Application	Acoustic transmission frequency	Outer length scale: single Fresnel zone ($\sim 50\lambda_0$)	Inner length scale: $\lambda_0/4$
SPACE08	12.5 kHz	6 m	3 cm
Small scale roughness	300 kHz	25 cm	1.25 mm
Swell / long wave features	1 kHz	75 m	37.5 cm

Fig. 5. Versatility in application of the surface profile reconstruction technique. The inner and outer length scales on surface reconstruction are determined by acoustic transmission frequency. Three transmission frequencies are considered and each corresponds to wave features of different characteristic scales. The range of wave features that can be resolved for each acoustic transmission frequency is also plotted on the dispersion relation curve for a gravity wave in 15 m deep water. This figure is adapted and modified from Fig. 11 in [1].

the robustness of the inversion algorithm, leads to the prospect of applying this acoustic remote sensing technique to an open ocean data set.

Since the inner and outer length scales on surface wave shape reconstruction are based on acoustic wavelength, the entire technique is scalable by acoustic transmission frequency. Depending on what type of waves are to be investigated, the transmission frequency can be chosen appropriately. For instance, high frequency acoustic pulses at 300 kHz as in the current experiment could be used to investigate small scale roughness or capillary effects. Open ocean surface scattering acoustic data has already been collected in the Surface Processes and Acoustic Communications Experiment (SPACE08) [1] at a transmission frequency of 12.5 kHz. This acoustic frequency corresponds to wave features between 3 cm and 6 m. Figure 5 shows three possible acoustic transmission frequency and their corresponding inner and outer length scales. Those length scales determine a range of wave features able to be investigated acoustically and is plotted on the dispersion relation curve for a gravity wave in 15 m deep water. Wave features greater in wavelength than the outer length will appear as a gross change in elevation in the reconstructed wave field. However, wave features less than the inner length scale will not be able to be resolved acoustically and will manifest as acoustic energy losses due to small scale roughness, where small in this context corresponds to a length of $\lambda_0/4$.

Experiments performed in the wave tank are highly controlled. The overhead wave field is very uniform in the along-crest direction, the acoustic propagation path is aligned with the source and receiver, and the overhead waves are very smooth. In contrast, the ocean environment will be less controlled and special care must be taken to deal with losses due to out of plane scattering, small scale roughness, and bubbles. Additionally, some improvements could be made to the inversion algorithm to further enhance the reconstruction of ocean waves. Currently reconstructed surface profiles are generated individually from independent surface reflected pulses. Because the surface profiles are gravity waves, they obey certain physics and information from a wave profile at one moment might be useful in the reconstruction of a wave profile at a different time. Using information from multiple acoustic pulses could be implemented by constraining the reconstructed profiles with a numerical wave model that uses prior information from surface wave shapes at different times.

ACKNOWLEDGMENT

We would like to acknowledge James Uyloan for his assistance in setting up the wave tank experiment and Dr. Dale Stokes for use of the MotionPro x3 camera.

REFERENCES

[1] G. B. Deane, J.C. Preisig, C. T. Tindle, A. Lavery, M.D. Stokes, "Deterministic forward scatter from surface gravity waves," J. Acoust. Soc. Am. 132, pp. 3673-3686, 2012.

[2] J. C. Preisig, G. B. Deane, "Surface wave focusing and acoustic communications in the surf zone," J. Acoust. Soc. Am. 116, pp. 2067-2080, 2004.

[3] S. P. Walstead, G. B. Deane, "Reconstructing surface wave profiles from reflected acoustic pulses," J. Acoust. Soc. Am. 134, pp. 2597-2611, 2013.

[4] M. V. Berry, "On deducing the form of surfaces from their diffracted echoes," J. Phys. A: Gen. Phys. 5, pp. 272-291, 1972.

[5] J. A. Ogilvy, "Wave scattering from rough surfaces," Rep. Prog. Phys. 50, pp. 1553–1608, 1987.

[6] E. I. Thorsos, "The validity of the Kirchhoff approximation for rough surface scattering using a Gaussian roughness spectrum," J. Acoust. Soc. Am. 83, pp. 78-92, 1988.